15. MolEN, An Interactive Structure Solution Procedure, Enraf-Nonius, Delft, Netherlands, 1990.
16. Geary, W. J. *Coord. Chem. Rev.* **1971**, *7*, 81.
17. Jeffery, J. C.; Thornton, P.; Ward, M. D. *Inorg. Chem.* **1994**, *33*, 3612.
18. Bonadies, J. A.; Kirk, M. L.; Lah, M. S.; Kessissoglou, D. P.; Hatfield, W. E.; Pecoraro, V. L. *Inorg. Chem.* **1989**, *28*, 2037.
19. Dutta, S.; Basu, P.; Chakravorty, A. *Inorg. Chem.* **1991**, *30*, 4031.

Photoresponsive Liquid Crystalline Copolymers Bearing a *p*-Methoxyazobenzene Moiety

Dong Hoon Choi, Suk Hoon Kang, Joon Youl Lee, and Asit Baran Samui*

Division of Textile, Chemical, and Industrial Engineering, Institute of Material Science and Technology, Kyung Hee University, Yongin-shi, Kyungki-do 449-701, Korea
**Naval Materials Research Laboratory, Naval Dockyard, Mumbai 400023, India*
Received May 15, 1998

Mesogenic and azo monomers were synthesized and copolymerized to obtain two copolymers composed of methacrylate and itaconate backbone. Glass transition temperatures of the copolymers were found to be slightly higher than ambient temperature. Both the copolymers showed liquid crystalline properties. *Trans-cis* isomerization in film state was observed under UV-irradiation with a light of 365 nm. Regarding the photochemical phase transition behavior, the transition rate of nematic-to-isotropic state was slightly faster in the methacrylate copolymer during irradiation at 365 nm and the rate of the reverse transition was much faster in itaconate copolymer under thermal effect.

Introduction

There is a considerable interest in the synthesis and characterization of azobenzene containing polymers for several reasons. These materials are found to possess unique optical properties.[1-7] In addition to the studies in the direction of nonlinear optical properties, there is constantly increasing attention in the field of optical data storage and holographic applications. Ikeda et. al. extensively studied the photochemically induced phase transition in polymer liquid crystals containing azobenzene.[8-12] Both azo homopolymers and azo-liquid crystalline (LC) copolymers have been found to be effective media for optical information storage. The mechanism of writing involves photoinduced excitation of the azobenzene group, which undergoes *trans-cis* isomerization. In the case of homopolymers, some extent of *cis* form remains even after thermal treatment. These molecules do not take part in further photochemical excitation and this is translated into birefringence.[13] In the case of azo-LC copolymers the process is different. Rod-like *trans* isomer fits into the LC environment whereas *cis* isomer disturbs it. On UV irradiation the *trans* form isomerizes to the *cis* form. This incident affects the LC environment, inducing a phase transition. LC phase is converted to an isotropic phase. This phenomenon can be used in a photo-recording system.[7]

Few reports appeared in the literature on azo-LC copolymer containing methoxy terminal unit with both comonomers. LC monomers containing the methoxy terminal unit mostly exhibit nematic texture. It was reported that photochemical phase transition is induced more easily in the least ordered nematic LC part compared to other textures of higher order.[10] Itaconate polymers, containing two azobenzene groups per monomer unit, have been found to possess enhanced nonlinear optical properties.[14] It was observed that there was a strong dipole interaction in the LC-itaconate azo copolymer system containing nitro terminal unit with azo part.[15] Similar copolymer having methoxy terminal group is expected to have much less dipole interaction. It seems, therefore, that it will be interesting to study the photochemical phase transition behavior of LC-itaconate azo copolymer containing methoxy terminal groups.

In the present study, we report the synthesis, characterization, *trans-cis* isomerization, photochemical phase transition behavior of methacrylate and itaconate copolymers with LC unit.

Experimental

Synthesis of monomers

4-methoxyphenyl-4'-methacryloyloxy hexyloxy benzoate (MMHB) (M-I). It was synthesized by following the method of Horvath *et al.*[16] using 4-hydroxy benzoic acid as the starting material.

^{1}H NMR (200 MHz, DMSO-d_6): δ (ppm) 8.01 (d, 2H, aromatic), 6.9-7.1 (m, 6H, aromatic), 5.99 (s, 1H, in $C\underline{H}_2$=), 5.63 (s, 1H, in $C\underline{H}_2$=), 4.08 (d, 4H, 2(O-$C\underline{H}_2$)), 3.74 (s, 3H, Ar-O$C\underline{H}_3$), 1.85 (s, 3H, αC-$C\underline{H}_3$), 1.39-1.72 (m, 8H, in -($C\underline{H}_2$)$_4$-).

4-methoxyphenyl methacryloyloxy hexyloxy azobenzene (MMHA) (M-II). 4-methoxy aniline was diazotized by standard technique and reacted with phenol at

0-5 °C over 48 hours. The product was purified by recrystallizing from the aqueous ethanol solution (H_2O: Ethanol=3 : 2, v/v). The azo compound thus formed was reacted with 6-chloro-1-hexanol to attach the spacer unit. In a typical composition, 0.01 mole of azo compound was reacted with 0.011 mole of 6-chloro-1-hexanol in presence of potassium carbonate and potassium iodide in dimethylformamide (DMF). The mixture was stirred for 20 hours at 90 °C. The solution was cooled to room temperature and the residue was removed by filtration. Recrystallization from the ethanol solution purified the product, 4'-(6-hydroxyhexyloxy)-4-methoxyazobenzene (HHMA). HHMA was reacted with methacryloyl chloride (mole ratio 1 : 1.3) in presence of triethylamine in tetrahydrofuran (THF) for 24 hours at 60 °C. The solution was cooled and excess methylene chloride was added. Repeated extractions were carried out with distilled water. The organic layer was separated and dried over anhydrous sodium sulfate. The solvent was evaporated under vacuum. Recrystallization from the ethanol solution purified the crude monomer. Yield. 60-65%

^{1}H NMR (200 MHz, DMSO-d_6): δ (ppm) 7.89 (m, 4H, aromatic), 6.98 (d, 4H, aromatic), 6.11 (s, 1H, in $C\underline{H}_2$=), 5.58 (s, 1H, in $C\underline{H}_2$=), 4.21 (t, 2H, -$C\underline{H}_2$-O), 4.08 (t, 2H, O-$C\underline{H}_2$-), 3.85 (s, 3H, Ar-O$C\underline{H}_3$), 1.95 (s, 3H, αC-$C\underline{H}_3$), 1.32-1.57 (m, 8H, in -($C\underline{H}_2$)$_4$-).

2-Methylene-succinic acid bis-(2{4-[2-(4-methoxy-phenyl)-azo]-phenoxy}-hexyl) ester (MSME) (M-III). 4'-(6-hydroxyhexyloxy)-4-methoxyazobenzene (HHMA) was synthesized as described above. It was then reacted with itaconic acid using Mitsunobu esterification method. 3.28 g (0.01 mole) of HHMA was dissolved in 50 mL THF. 6.55 g (0.025 mole) of triphenyl phosphine, dissolved in 10 mL THF, was added. The solution was stirred under argon at room temperature. A solution containing 4.04 g (0.02 mole) of diisopropyl azodicarboxylate and 0.72 g (0.0055 mole) of itaconic acid in 10 mL THF was added dropwise over a period of 40 minutes. The progress of the reaction was checked by thin layer chromatography (TLC). The reaction was completed in 2 hours. The solution was cooled in a deep freezer and filtered. The residue was recrystallized from acetonitrile to get pure product. Yield. 55%

^{1}H NMR (200 MHz, DMSO-d_6): δ (ppm) 7.87 (m, 8H, aromatic), 6.97 (m, 8H, aromatic), 6.32 (s, 1H, in $C\underline{H}_2$=), 5.71 (s, 1H, in $C\underline{H}_2$=), 4.15 (m, 4H, -$C\underline{H}_2$-O), 4.01 (t, 4H, O-$C\underline{H}_2$-), 3.82 (s, 6H, Ar-O$C\underline{H}_3$), 3.34 (s, 2H, αC-$C\underline{H}_2$-), 1.44-1.82 (m, 16H, in -($C\underline{H}_2$)$_4$-).

Synthesis of copolymers. Monomer I (M-I) and Monomer II (M-II) were dissolved in freshly distilled N-methylpyrrolidone (NMP) to a concentration of 0.4 mole/l. The solution was transferred into a two-necked flask and placed in a thermostated oil bath maintained at 70 °C. The solution was freed from oxygen by purging argon gas for 2 hours. Azobisisobutyronitrile (AIBN) (2 mole% with respect to total monomer) was added in two equal installments at an interval of 24 hours. The solution was stirred for 48 hours, cooled to room temperature, and then poured in hot ethanol. The yellow solid was filtered and then reprecipitated from THF solution into *n*-hexane/diethyl ether (4 : 1, v/v). The pure copolymer was finally dried for 48 hours at 60 °C under vacuum. Copolymer II (CP II) was also prepared by the same method.

Characterization

NMR Spectroscopy. Proton NMR spectra were recorded on Varian 200 NMR spectrometer using tetramethylsilane as an internal standard and chloroform-d ($CDCl_3$) as a solvent. NMR peak integration method was used to determine the copolymer compositions.

UV/VIS Spectroscopy. Hewlett Packard (model 8453) spectrophotometer was employed to record the UV/VIS spectra. Both the copolymer solutions (in THF) and films were examined. The films were prepared by spin coating from 2-5% copolymer solution in THF. The films were then dried under vacuum at 60 °C for 24 hours. The solution taken into a quartz cell or copolymer film coated on a glass slide was placed within the UV/VIS spectrophotometer. The samples were irradiated with a UV lamp (8 watt) from a distance of 8 cm and the absorption spectra were recorded simultaneously.

Gel Permeation Chromatography. The number average molecular weight (M_n) and molecular weight distribution were determined by using Waters gel permeation chromatograph (model 440) attached with 410 diffraction refractometer. Spectral grade THF was used as the solvent and molecular weight calibration was done using polystyrene standard.

Differential Scanning Calorimetry. Transition temperatures were measured using a differential scanning calorimeter (Perkin Elmer, DSC 4) at a scan rate of 10 °C/min under nitrogen atmosphere. Both heating and cooling scans were repeated three times.

Photochemical Phase Transition Behavior. The copolymer thin films were spin coated on the glass slide which was precoated with uniaxially rubbed polyimide. The sample was placed on a hot stage and irradiated with a UV lamp (365 nm, 8 W) placed at a distance of 10 cm. He-Ne laser, falling in perpendicular direction to the sample surface, was used as probe beam. The first polarization axis was set to 45° to the rubbing direction of polyimide substrate to observe the highest birefringence of LC film. The laser beam was focused on the film surface through a polarizer and the transmitted light was allowed to fall on detector after passing through an analyzer. The change in transmittance of He-Ne laser was recorded *in-situ* by using photodiode which in-turn was connected to a lock-in ampli-

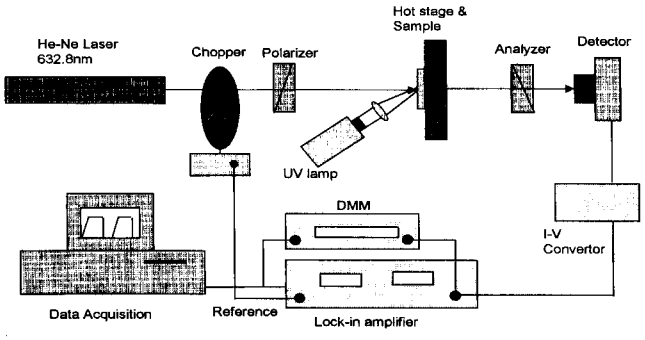

Scheme 1. Schematic diagram of optic setup for photochemical phase transition.

fier with 1 kHz reference signal from a mechanical chopper. (See Scheme 1)

Results and Discussion

Synthetic procedure and copolymer structures are depicted in Scheme 2 and 3. Copolymer I (CP I) consists of MMHB and MMHA units, whereas copolymer II (CP II) consists of MMHB and MSME units. All the copolymers are yellow in color and well soluble in organic solvents such as tetrahydrofuran, dimethylformamide, chloroform, acetone etc. The details about monomer feeding ratio, copolymer composition,

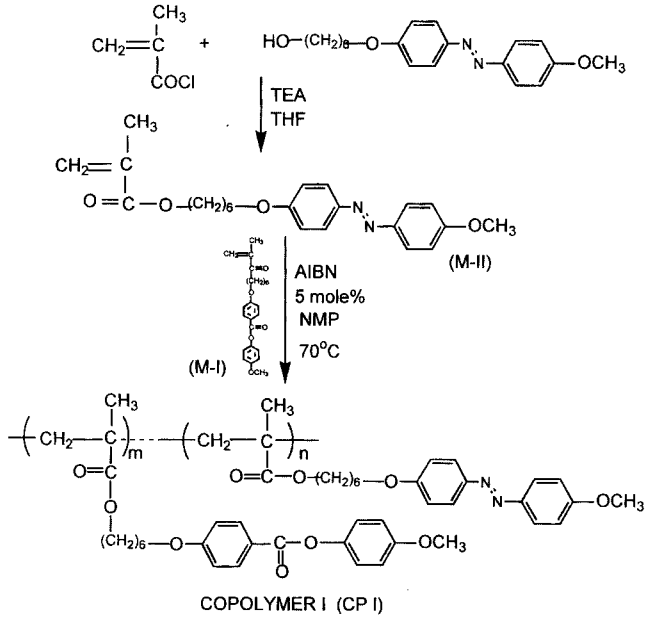

Scheme 2. Synthetic procedure for LC copolymer I.

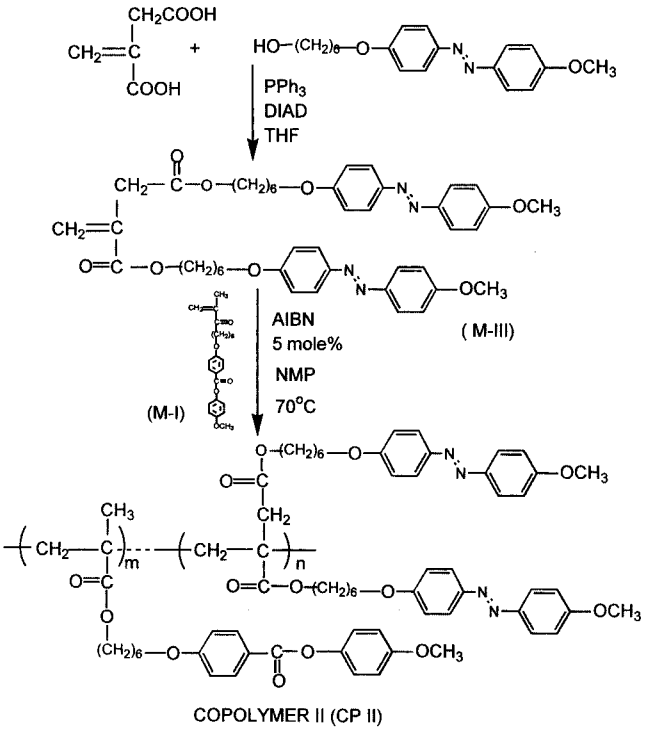

Scheme 3. Synthetic procedure for LC copolymer II.

Table 1. Compositions and moelcular weights of two copolymers

Sample	Monomer Feeding Mole Ratio	Resultant Mole Ratio	M_n	Polydispersity
CP I	M I:M II	M I:M II	14328	2.5034
CP II	M I:M III	M I:M III	11154	1.5032

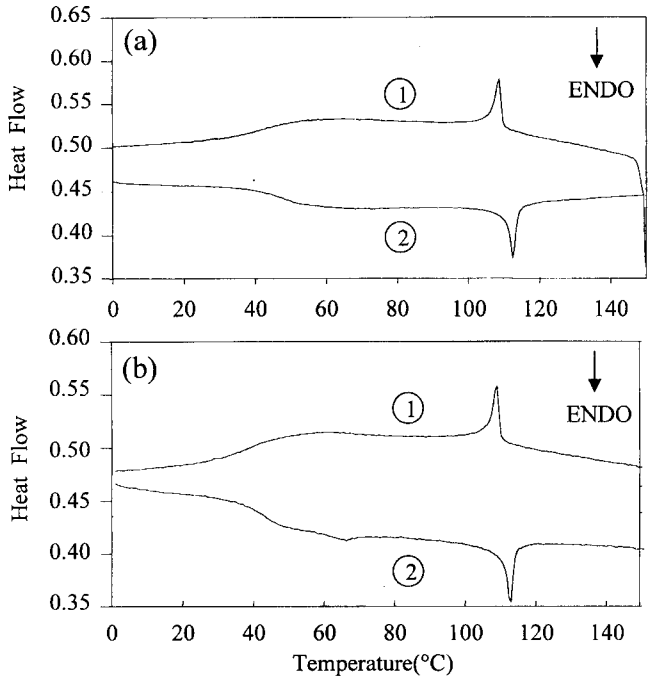

Figure 1. DSC thermograms of two copolymers. ((a) CP I; (b) CP II; ① cooling; ② heating)

and molecular weight are listed in Table 1. The molecular weights (M_n) of copolymers are in the range of 11,000 to 15,000 that is suitable for studying the photochemical phase transition and liquid crystalline behavior.

Liquid Crystalline Transition. Figure 1 shows the representative DSC thermograms of copolymers ((a) CPI, (b) CP II). The base line shift indicates the glass transition temperature (T_g). The temperature (T_{NI}) of nematic-to-isotropic transition was clearly observed. Table 2 presents the thermal transition temperatures of the monomers and copolymers. Glass transition temperatures of two copolymers are very close to the ambient temperature. The LC texture was found to disappear at T_{NI} and reappear during cooling around the same temperature. The textures were confirmed

Table 2. Transition temperatures of monomers and copolymers obtained from DSC thermograms

	Crystalline melting temperature (T_{cr} °C)	Glass transition temperature (T_g °C)	Isotropization temperature (T_{NI} °C)
MMHB (M I)	37	–	45
MMHA (M II)	62	–	85
MSME (M III)	108	–	150
CP I (M I/M II)	–	37	104
CP II (M I/M II)	–	36	111

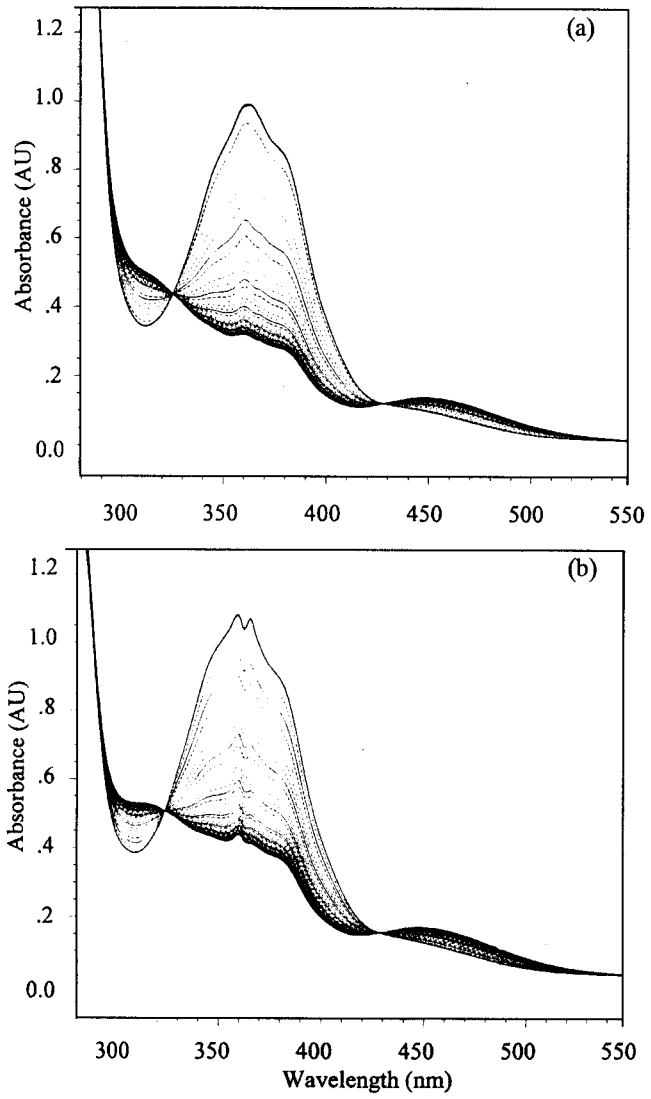

Figure 2. UV-VIS spectra of copolymers during irradiation at 365 nm. ((a), CP I; (b), CP II)

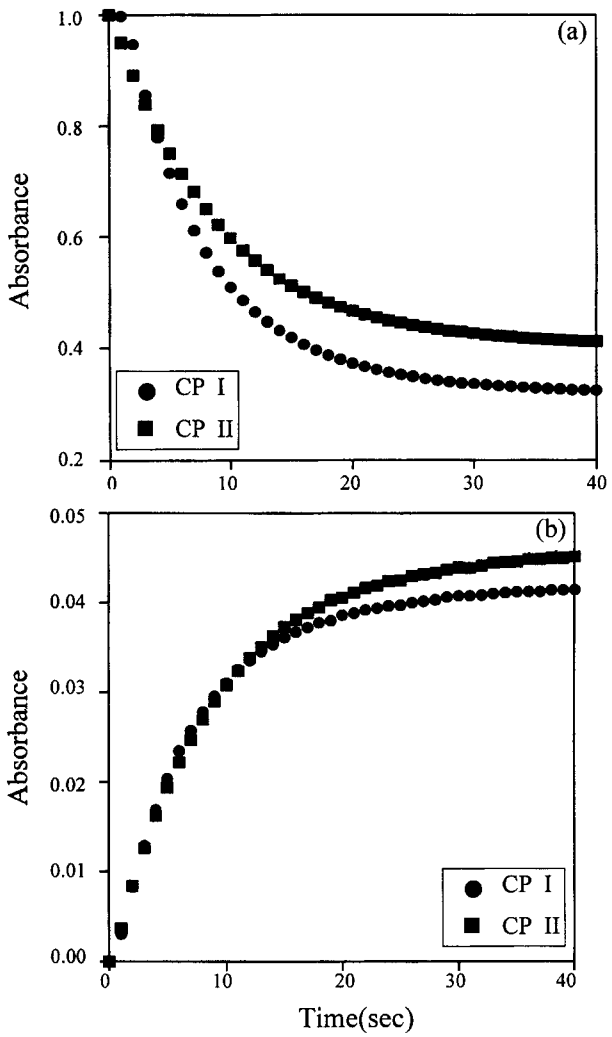

Figure 3. The change of absorbance during irradiation at 365 nm. ((a), 365 nm; ((b) 450 nm)

to be nematic in all the monomers and copolymers by polarized optical microscopy.

Photoisomerization Behavior. Both the monomers and copolymers were found to undergo isomerization in both solution and film states under irradiation with a UV source. The thicknesses of the films of CP I and CP II were determined to be 0.27 and 0.33 μm respectively by using Tencor P10. Figure 2 shows the representative electronic spectra of copolymer in film state ((a) CP I, (b) CP II), which are taken at 1 sec interval. The absorbance (π-π^* transition) at 365 nm is reduced while the absorbance (n-π^* transition) at 450 nm is increased during irradiation, as *trans* form gradually isomerizes to *cis* form. Two typical isobestic points can be observed around 330 and 430 nm respectively. Figure 3 shows the change of absorbance at 365 nm (a) and 450 nm (b) during irradiation for copolymer films. In order to compare the rates of isomerization in two copolymers, we set the same distance between the sample and the UV lamp. The light was isolated with the 365 bandpass filter (light intensity 2.5 mW/cm^2). The rate of photoisomerization from *trans* to *cis* form in CP I is observed to be faster than that of CP II. Slow rate of photoisomerization in CP II could be attributed to the geometrical hindrance of the azo molecules in the itaconate repeating unit.

Photochemical Phase Transition. During irradiation with a UV source, the *trans* form of the azobenzene unit isomerizes to *cis* form. *Cis* form destabilizes the LC phase of the copolymer, inducing phase transition to an isotropic phase. In the case of two copolymers, nematic-to-isotropic transformation can be performed over ten cycles at each temperature without any hysteresis, which is due to *trans*-to-*cis* conformational change. During the photochemical processes, there is a change in birefringence of the LC films. The phase transition experiments were carried out at temperatures below T_{NI}. In order to investigate the photochemical nematic-to-isotropic transition quantitatively, we selected a reduced temperature (T_{red}) to compare the phase transition behavior. The reduced temperature (T_{red}) was calculated dividing the measuring temperature, T (K) by nematic-to-isotropic transition temperature, T_{NI} (K). When T_{red} is equal to unity, that will be the nematic-to-isotropic transtion temperature. The response time (τ_1) was defined as the time required to reduce the transmittance across the polarizers to 36.7% (1/e × 100) of the maximum transmittance. τ_2 was

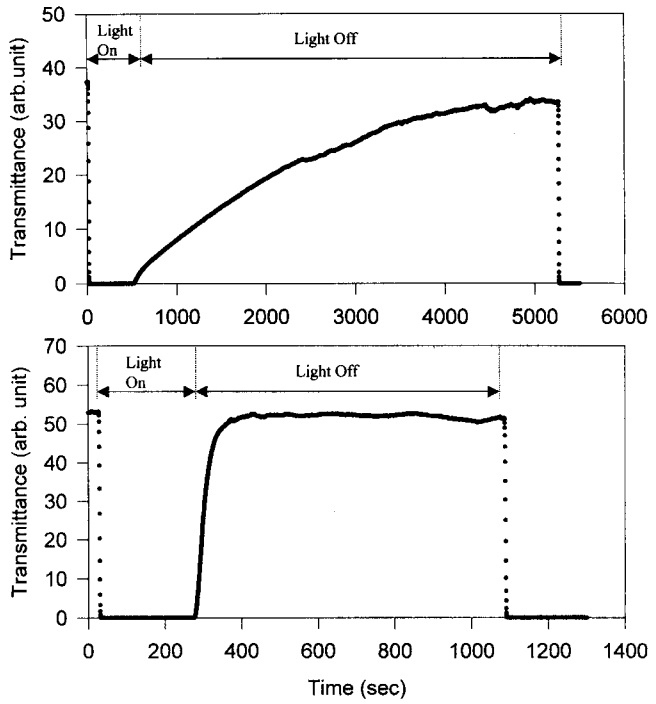

Figure 4. Photochemical nematic-to-isotropic transition and thermal isotropic-to-nematic transition of two copolymers. ((a) CP I; (b) CP II)

also defined as the time required for the transmittance to reach to 67.3% of the saturated one. Figure 4 shows the representative growth and decay curve of transmittance during irradiation and dark phases at the same T_{red} (=0.968) for CP I and CP II.

As expected, the rate of nematic-to-isotropic phase transition is much larger than that of isotropic-to-nematic phase transition arising from thermal effect. When we compared the rates of nematic-to-isotropic phase transition of two copolymers, the rate of CP I is observed slightly larger. This is consistent with the result from photoisomerization behavior at room temperature. However, the rate of isotropic-to-nematic phase transition of CP II is much larger than that of CP I. First of all, the response times (τ_1, sec) between two copolymers were shown with the change of the reduced temperature, T_{red} in Figure 5. In a whole range of T_{red} described here, τ_1 in CP I is smaller than that in CP II. This implies that the azobenzene unit in CP I was randomly distributed in polymer structure so that the *cis* transition can enhance the disruption of LC phase. In the case of itaconate copolymer (CP II), the same number of *azo* molecules resided to be localized in the half of the repeating units of methacrylate copolymer (CP I). The number of LC monomer (M I) in CP II is larger than that in CP I. Therefore, the isolated LC domains formed with monomer I (nematogenic LC monomer) are predominant and were perturbed much slowly resulting from the *trans*-to-*cis* transformation of azobenzene unit.

We can calculate the response time, τ_2 at each T_{red} in two copolymers after turning off the UV light. (See Figure 6) With an increase of reduced temperature, τ_2 becomes smaller as we expected. In all T_{red} range, the transition rate (τ_2) for CP II is much faster than that for CP I. This indicates that

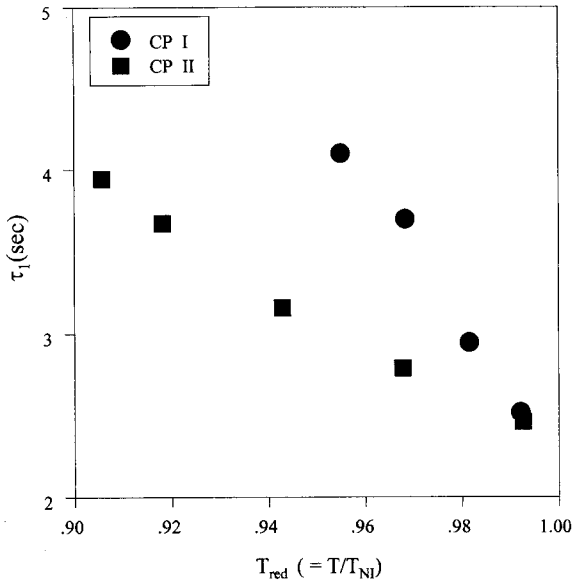

Figure 5. Relationship between the response time (τ_1) of nematic-to-isotropic transition and the reduced temperatures.

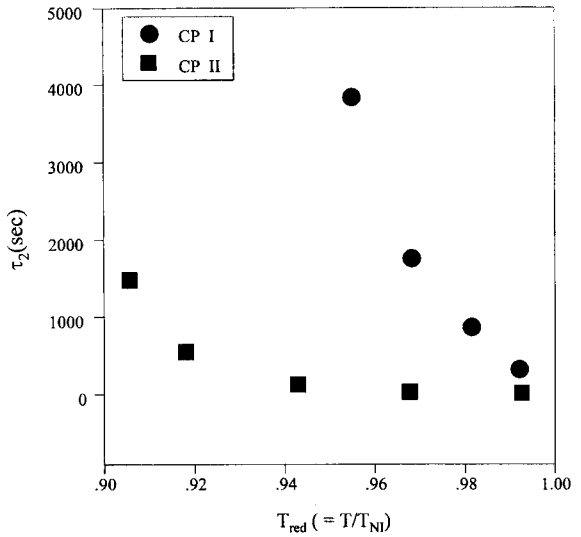

Figure 6. Relationship between the response time (τ_2) of isotropic-to-nematic transition and the reduced temperatures.

the isolated LC monomers (M I) rapidly gathered to rebuild the well-organized small LC domain to increase the birefringence. In the final stage of recovery, the vicinal portions of M I to azobenzene moiety and transformed *trans* form were slowly crystallized cooperatively to be involved in the pre-built LC domain. Finally the transmittance was saturated to the initial value. In CP I, the slow recovery rate is ascribed to the delayed process of *cis*-to-*trans* transformation and then every vicinal LC unit (M I) was interacted each other. The vicinal LC units to azo group cannot gather to organize the LC domain only. Those molecules should be delayed to involve in the crystalline phase until the *cis* form was transformed to *trans* LC form. Therefore, the response time is much larger than that in CP II.

The reverse reaction was controlled only by thermal effect. We tried to estimate how much thermal energy is needed for the isotropic-to-nematic transition per molecular concentra-

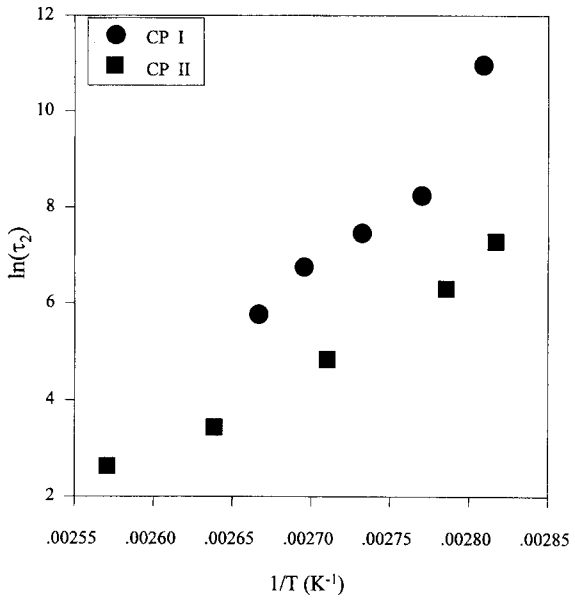

Figure 7. Arrhenius Relationship between the logarithmic response time of isotropic-to-nematic transition and the measured temperatures.

tion. Relationship between the logarithmic second response time (ln τ_2) and the reciprocal measuring temperature (1/T) is shown in Figure 7. We could obtain the slope of the curve to calculate the activation energy (E_a kcal/mole) in the repect of Arrhenius behavior. The calculated activation energies were 67 kcal/mole and 30 kcal/mole for CP I and CP II, respectively. This information is quite well consistent with previous explanation why the reverse rate in CP II is much larger than that in CP I.

Conclusion

In the present study, we could synthesize two different types of copolymer bearing an azobenzene chromophore in the side chain. We evaluated the photoisomerization and photochemical phase transition behaviors of two types of liquid crystalline copolymer with different repeating unit and almost same number of azobenzene unit in single polymer chain. We could observe the isothermal photochemical nematic-to-isotropic transition behavior arising from *trans-cis* photoisomerization. The response time, from nematic-to-isotropic phase in CP I is slightly smaller that that in CP II. On the other hand, the reverse reponse time for isotropic-to-nematic phase transition in CP II is much smaller than that in CP I. All the photochemical phase transition was affected by *trans-cis* photoisomerization to vary the response times. The effect of structure of copolymer on phase transition was attributed to the stabilization of LC molecular alignment of the side chain mesogen in the nematic phase by different repeating unit.

Acknowledgment. This work was supported by KOSEF (contract#: 96-0300-10-03-3).

References

1. Ringsdorf, H.; Schmidt, H. W. *Makromol. Chem.* **1984**, *185*, 1327.
2. Whitehurst, C.; Shaw, D. J.; King, T. A. *Proceedings of the International Society for Optical Engineering, Sol-Gel Optics*, Mackenzie, J. D. and Donald, R. U., Eds. SPIE, Washington DC, 1990; Vol.1328, p 183.
3. Dunn, B.; Mackenzie, J. D.; Zink, J. I.; Stafsudd, O. M. *Proceedings of the International Society for Optical Engineering, Sol-Gel Optics*, Mackenzie, J. D. and Donald, R. U., Eds. SPIE, Washington DC, 1990; Vol. 1328, p 174.
4. Sasaki, T.; Ikeda, T.; Ichimura, K. *Macromolecules* **1992**, *25*, 3807.
5. Rochon, P.; Gosselin, J.; Natansohn, A.; Xie, S. *Appl. Phys. Lett.* **1992**, *4*, 60.
6. Natansohn, A.; Rochon, P.; Gosselin, J.; Xie, S. *Macromolecules* **1992**, *25*, 2268.
7. Hayashi, T.; Kawakami, H.; Doke, Y.; Tsuchida, A.; Onogi, Y.; Yamamoto, M. *Eur. Polym. J.* **1995**, *31*(1), 23.
8. Ikeda, T.; Horiuchi, S.; Karanjit, D. B.; Kurihara, S.; Tazuke, S. *Macromolecules* **1990**, *23*, 36.
9. Ikeda, T.; Horiuchi, S.; Karanjit, D. B.; Kurihara, S.; Tazuke, S. *Macromolecules* **1990**, *23*, 42.
10. Ikeda, T.; Horiuchi, S.; Karanjit, D. B.; Kurihara, S.; Tazuke, S. *Macromolecules* **1990**, *23*, 3938.
11. Kurihara, S.; Ikeda, T.; Sasaki, T.; Kim, H. B.; Tazuke, S. *Macromolecules* **1990**, *24*, 627.
12. Kurihara, S.; Ikeda, T.; Sasaki, T.; Kim, H. B.; Tazuke, S. *Mol. Cryst. Liq. Cryst.* **1991**, *195*, 251.
13. Natansohn, A.; Xie, S.; Rochon, P. *Macromolecules* **1992**, *25*, 5531.
14. Song, S.; Choi, D. H.; Lim, S. J.; Jahng, W. S.; Kim, N. *Bull. Korean Chem. Soc.* **1997**, *18*(3), 256.
15. Samui, A. B.; Kang, S. H.; Choi, D. H. *J. Appl. Polym. Sci.* submitted 1998.
16. Horvath, J.; Nyitrai, K.; Cser, F.; Hardy, G. Y. *Eur. Polym. J.* **1985**, *21*(3), 251.